

# Human and climate impacts on the 21st century hydrological drought



N. Wanders\*, Y. Wada

Department of Physical Geography, Faculty of Geosciences, Utrecht University, Utrecht, The Netherlands

## ARTICLE INFO

### Article history:

Available online 29 October 2014

### Keywords:

Hydrological drought  
Human water use  
Climate change  
Reservoirs  
Drought characteristics  
PCR-GLOBWB

## SUMMARY

Climate change will very likely impact future hydrological drought characteristics across the world. Here, we quantify the impact of human water use including reservoir regulation and climate change on future low flows and associated hydrological drought characteristics on a global scale. The global hydrological and water resources model PCR-GLOBWB is used to simulate daily discharge globally at 0.5° resolution for 1971–2099. The model was forced with the latest CMIP5 climate projections taken from five General Circulation Models (GCMs) and four emission scenarios (RCPs), under the framework of the Inter-Sectoral Impact Model Intercomparison Project.

A natural or pristine scenario has been used to calculate the impact of the changing climate on hydrological drought and has been compared to a scenario with human influences. In the latter scenario reservoir operations and human water use are included in the simulations of discharge for the 21st century. The impact of humans on the low flow regime and hydrological drought characteristics has been studied at a catchment scale.

Results show a significant impact of climate change and human water use in large parts of Asia, Middle East and the Mediterranean, where the relative contribution of humans on the changed drought severity can be close to 100%. The differences between Representative Concentration Pathways are small indicating that human water use is proportional to the changes in the climate. Reservoirs tend to reduce the impact of drought by water retention in the wet season, which in turn will lead to increased water availability in the dry season, especially for large regions in Europe and North America. The impact of climate change varies throughout the season for parts of Europe and North-America, while in other regions (e.g. North-Africa, Middle East and Mediterranean), the impact is not influenced by seasonal changes.

This study illustrates that the impact of human water use and reservoirs is nontrivial and can vary substantially per region and per season. Therefore, human influences should be included in projections of future drought characteristics, considering their large impact on the changing drought conditions.

© 2014 Elsevier B.V. All rights reserved.

## 1. Introduction

Climate change is expected to increase drought intensity and frequency worldwide as a result of change in precipitation patterns and rising temperature (Burke et al., 2006; Lehner et al., 2006; Feyen and Dankers, 2009; Dai, 2011; Dai, 2013; Prudhomme et al., 2014; Trenberth et al., 2014). Drought is generally related to meteorological extremes and is induced by below-normal precipitation (Wilhite and Glantz, 1985; Wilhite, 2000; Mishra and Singh, 2010). Lack of precipitation causes meteorological drought and agricultural drought over the region, but further propagates into hydrological drought via the drainage network (Tallaksen et al., 1997; Sheffield and Wood, 2007; Tallaksen et al., 2009; Sheffield et al., 2012; Van Loon et al., 2014). Various studies

analysed the severity, frequency and trends of hydrological droughts using large-scale hydrological models that enable the analysis of drought over continental to global scales (Hisdal et al., 2001; Fleig et al., 2006; Feyen and Dankers, 2009; Tallaksen et al., 2009; Corzo-Perez et al., 2011; Van Huijgevoort et al., Jul. 2013; Van Huijgevoort et al., 2014; Alderlieste et al., 2014). However, the anthropogenic impact on drought is generally less well known and such impact has rarely been explored. Few exceptions are recent studies by Dai (2011), Dai (2013) and Sheffield et al. (2012) who indicated that anthropogenic global warming is likely responsible for intensifying meteorological droughts, primarily due to enhanced evaporative demand and altered monsoon circulation over regions such as Africa and Asia. Another exception by Wada et al. (2013) showed that human water consumption substantially intensifies the magnitude of hydrological droughts regionally by 10–500%, and it alone increases global drought frequency by 30%. However, no study

\* Corresponding author.

E-mail address: [n.wanders@uu.nl](mailto:n.wanders@uu.nl) (N. Wanders).

has yet provided a comprehensive overview of human and climate impacts on future hydrological drought at the global scale. Prudhomme et al. (2014) provided future projections of hydrological drought based on a large ensemble of five Global Climate Models (GCMs) from the latest CMIP5 (Coupled Model Intercomparison Project Phase 5), four emission scenarios or Representative Concentration Pathways (RCPs) and seven Global Hydrological Models (GHMs). Yet, they considered only the effect of climate on hydrological drought using the streamflow simulated under natural or pristine conditions such that anthropogenic influence (e.g., irrigation and reservoir regulation) on resulting drought is not explicitly incorporated.

The severe impacts of large-scale droughts have historically showed the need to improve understanding of drought mechanisms so that our society can be better prepared (Trenberth et al., 1988; Gleick, 2000; Andreadis et al., 2005; Seager, 2007; Gleick, 2010; Pederson et al., 2012). Thus, providing a comprehensive overview of future drought projections considering both human and climate impacts is a vital step, ensuring future water and food security. Here, we present for the first time a full global analysis of the impact of human activities (irrigation and reservoir regulation, Wada et al., 2013) and climate change on hydrological drought. We simulated streamflow both under natural or pristine conditions and under conditions including human influences using the global hydrological and water resources model PCR-GLOBWB (Van Beek et al., 2011; Wada et al., 2011; Wada et al., 2011; Wada et al., 2014) with five GCMs from the latest CMIP5 and four emission scenarios (here represented by RCPs 2.6, 4.5, 6.0 and 8.5). We incorporate human-induced change by including human water use for irrigation and reservoir regulation parameterized by the latest extensive global reservoir data set (GRanD, Lehner et al., May 2011). Another innovative aspect of this study is that we apply a transient spatially-distributed threshold or  $Q_{90}$  (30-year window) identifying drought characteristics that reflects changes in the hydrological regime over time (Wanders et al., 2014), while most studies used the threshold calculated over the control or historical period (e.g., 1971–2000). A transient threshold assumes adaptation to long-term changes in the hydrological regime as the drought is defined by a deviation from normal conditions (i.e. normal implies decadal updated 30-year averages according to the WMO guidelines) (World Meteorological Organization, 2007; Arguez and Vose, 2010). Our study stands out from earlier work by presenting for the first time the human impact on future hydrological droughts using the latest multi-model climate projections and multi-emission scenarios.

Section 2 of this paper presents a brief description of the global hydrological and water resources model PCR-GLOBWB, climate forcing data, the drought identification method and the simulation protocol. In Section 3 the simulation results are presented and the human and climate impacts on future hydrological drought are evaluated globally and per river basin. Section 4 discusses the advantages and the limitations of our approach and the associated uncertainties, and provides conclusions from this study.

## 2. Material and methods

### 2.1. Model simulation of streamflow

The state-of-the-art global hydrological and water resources model PCR-GLOBWB was used to simulate spatial and temporal continuous fields of discharge and storage in rivers, lakes, and wetlands at a 0.5° spatial resolution (Wada et al., 2010; Van Beek et al., 2011; Wada et al., 2014). In brief, the model simulates for each grid cell and for each time step (daily) the water storage in two vertically stacked soil layers and an underlying groundwater layer. At the top a canopy

with interception storage and a snow cover may be present. Snow accumulation and melt are temperature driven and modelled according to the snow module of the HBV model (Bergström, 1995). To represent rain-snow transition over sub-grid elevation dependent gradients of temperature, 10 elevation zones were distinguished in each grid cell based on the HYDRO1k Elevation Derivative Database (<https://lta.cr.usgs.gov/HYDRO1K/>), and scaled the 0.5° grid temperate fields with a lapse rate of 0.65 °C per 100 m. The model computes the water exchange between the soil layers, and between the top layer and the atmosphere (rainfall, evaporation and snowmelt). The third layer represents the deeper part of the soil that is exempt from any direct influence of vegetation, and constitutes a groundwater reservoir fed by active recharge. The groundwater store is explicitly parameterized and represented with a linear reservoir model (Kraijenhof van de Leur, 1962). No lateral flow is included in the groundwater store at the global scale, however this has been implemented successfully on a regional scale (Sutanudjaja et al., 2014). Sub-grid variability is considered by including separately short and tall natural vegetation, open water (lakes, floodplains and wetlands), soil type distribution (FAO Digital Soil Map of the World), and the area fraction of saturated soil calculated by the Improved ARNO scheme (Hagemann and Gates, 2003) as well as the spatio-temporal distribution of groundwater depth based on the groundwater storage and the surface elevations as represented by the 1 km by 1 km HYDRO1k data set. Simulated specific runoff from the two soil layers (direct runoff and interflow) and the underlying groundwater layer (base flow) is routed along the river network based on the Simulated Topological Networks (STN30, Vörösmarty et al., 2000) using the method of characteristic distances (Wada et al., 2014).

The PCR-GLOBWB model and model outputs have been extensively validated in earlier work. Simulated mean, minimum, maximum, and seasonal flow, monthly actual evapotranspiration, and monthly total terrestrial water storage were evaluated against 3600 GRDC observations (<http://www.bafg.de/GRDC>) ( $R^2 \sim 0.9$ ), the ERA-40 reanalysis data, and GRACE satellite observations, respectively in earlier work (Van Beek et al., 2011; Wada et al., 2012; Wada et al., 2014), and generally showed good agreement. Simulated drought deficit volumes were also validated against those derived from observed streamflow (from GRDC stations) for major river basins of the world (Wada et al., 2013). The comparison generally showed reasonable agreement for most of the basins, which leads to the conclusion that PCR-GLOBWB can adequately reproduce low flow conditions and associated drought events across the globe.

The model was forced with daily fields of precipitation, reference (potential) evapotranspiration and temperature taken from five GCMs (Table 1) and four underlying emission scenarios (here accounted for by using four RCPs (Table 2)). The newly available CMIP5 climate projections were obtained through the Inter-Sectoral Impact Model Intercomparison Project (Warszawski et al., 2014). The GCM climate forcing was bias-corrected on a grid-by-grid basis (0.5° grid) by scaling the long-term monthly means of the GCM daily fields to those of the observation-based WATCH climate forcing for the overlapping reference climate 1960–1999 (Hempel et al., 2013). Potential evapotranspiration was calculated

**Table 1**  
GCMs (Global Climate Models) used in this study.

GCM	Organization
HadGEM2-ES	Met Office Hadley Centre
IPSL-CM5A-LR	Institute Pierre-Simon Laplace
MIROC-ESM-CHEM	JAMSTEC, NIES, AORI (The University of Tokyo)
GFDL-ESM2M	NOAA Geophysical Fluid Dynamics Laboratory
NorESM1-M	Norwegian Climate Centre

**Table 2**

Overview of Representative Concentration Pathways (RCPs) (Van Vuuren et al., 2011). Radiative forcing values include the net effect of all anthropogenic greenhouse gases and other forcing agents.

RCP	Scenario
2.6	Peak in radiative forcing at $\sim 3.1 \text{ W m}^2$ ( $\sim 490 \text{ ppm CO}_2$ equivalent) before 2100 and then decline (the selected pathway declines to $2.6 \text{ W m}^2$ by 2100)
4.5	Stabilization without overshoot pathway to $4.5 \text{ W m}^2$ ( $\sim 650 \text{ ppm CO}_2$ equivalent) at stabilization after 2100
6.0	Stabilization without overshoot pathway to $6 \text{ W m}^2$ ( $\sim 850 \text{ ppm CO}_2$ equivalent) at stabilization after 2100
8.5	Rising radiative forcing pathway leading to $8.5 \text{ W m}^2$ ( $\sim 1370 \text{ ppm CO}_2$ equivalent) by 2100

with the bias-corrected GCM climate forcing with the method of Hamon (1963). The resulting bias-corrected transient daily climate fields were used to force the model over the period 1971–2099 with a spin-up, reflecting a climate representative prior to the start of the simulation period. The results of each GCM are treated equally and no weight was given to a particular GCM based on the performance against historic climate. As a result, 20 projections (5 GCMs with 4 RCPs) of future daily streamflow were produced.

## 2.2. Drought calculation

Hydrological drought characteristics (e.g. drought duration and deficit volume) were derived from simulated time series of daily discharge ( $Q$ ) using the variable threshold level approach (e.g. Yevjevich, 1967; Dracup et al., April 1980; Tallaksen et al., 1997; Hisdal et al., 2004; Fleig et al., 2006; Tallaksen et al., 2009; Wanders et al., 2010). In this study the  $Q_{90}$  ( $\text{m}^3 \text{ s}^{-1}$ ) was derived from the flow duration curve, where the  $Q_{90}$  is the threshold which is equalled or exceeded for 90% of the time. This threshold has been selected to study the impact of severe drought conditions and has been used in multiple studies where drought is studied for future and current hydrological conditions (e.g. Fleig et al., 2006; Parry et al., 2010; Wanders and Van Lanen, 2013; Van Loon et al., 2014).

The drought state is given by:

$$Ds(t, n) = \begin{cases} 1 & \text{for } Q(t, n) < Q_x(t, n) \\ 0 & \text{for } Q(t, n) \geq Q_x(t, n) \end{cases} \quad (1)$$

where  $Q_x(t, n)$  is the threshold which is equalled or exceeded for  $x$  percent of the time and  $Ds(t, n)$  is a binary variable indicating if a location or grid cell ( $n$ ) is in drought at a given time  $t$ . The drought duration for each event at  $n$  is calculated with:

$$Dur_{i,n} = \sum_{t=S_i}^{L_i} Ds(t, n) \quad (2)$$

where  $Dur_{i,n}$  is the drought duration ( $d$ ) of event  $i$  at  $n$ ,  $S_i$  the first time step of a event  $i$  and  $L_i$  the last time step of the event. An event starts when  $Q(t, n) < Q_x(t, n)$  and ends when  $Q(t, n) \geq Q_x(t, n)$ . The deficit volume per time step was defined by:

$$Def(t, n) = \begin{cases} Q_x(t, n) - Q(t, n) & \text{for } Ds(t, n) = 1 \\ 0 & \text{for } Ds(t, n) = 0 \end{cases} \quad (3)$$

where  $Def(t, n)$  is the daily deficit volume of drought  $i$  ( $\text{m}^3 \text{ s}^{-1}$ ) at  $n$ . The total drought deficit volume for each drought event was calculated with:

$$Def_i(n) = \sum_{t=S_i}^{L_i} Def(t, n) \quad (4)$$

where  $Def_i(n)$  is the total deficit volume of the drought event  $i$  ( $\text{m}^3 \text{ s}^{-1}$ ) at  $n$ . The deficit volume is the cumulative deviation of

the discharge from the threshold over the duration of a drought event. The intensity of all drought events is calculated with:

$$Int(n) = \sum_{i=1}^I \frac{Def_i(n)}{Dur_i(n)} \quad (5)$$

where the total drought deficit is divided by the total drought duration of location  $n$ , for all drought events  $i$ , to obtain the total drought intensity ( $\text{m}^3 \text{ s}^{-1} \text{ d}^{-1}$ ). The intensity enables comparison of the drought impact for a location under different scenarios. If the  $Q_x(t, n)$  equals  $0 \text{ m}^3 \text{ s}^{-1}$  by definition a drought will not occur since  $Ds(t, n)$  will remain zero (Eq. 1). If  $Q_x(t, n)$  equals  $0 \text{ m}^3 \text{ s}^{-1}$  for more than 50% of the time, no drought characteristics were calculated for this cell, although some techniques exist to deal with these extreme situations (Van Huijgevoort et al., 2012). In this study these locations were excluded from the analysis, since frequent zero discharge situations are part of the local climate (i.e. aridity) and are not manifestation of hydrological drought condition or occurrence.

## 2.3. Transient variable threshold approach

Most studies that evaluate future changes in hydrological drought use the Variable Threshold level Method (VTM), to derive drought characteristics (e.g. Prudhomme et al., 2014; Alderlieste et al., 2014; Forzieri et al., 2014). In this study, we used transient Variable Threshold level Method approach ( $VTM_t$ ) developed by Wanders et al. (2014). The  $VTM_t$  was calculated from the daily values of  $Q_x$  derived from simulated discharge of the previous 30-year period ( $x = 90$ , in this study). For each month, daily discharge values of the last 30-year period were binned and the  $Q_x$  was calculated. Thereafter, the monthly values of  $Q_x$  were smoothed with a moving average window of 30-days, resulting in the variable threshold ( $VTM_t$ ). The  $VTM_t$  is expected to adapt to changes in the hydrological regime, based on the simulation of the previous 30-year period, while the standard VTM does not change over time and is normally derived from a control period (typically 1970–2000). Present climatology can significantly change over the future period under human and climatological influences. This will result in an altered hydrological regime and therefore the  $VTM_t$  was used when future hydrological drought characteristics were calculated. This requires that the  $VTM_t$  is calculated every day and dependent on the climatology of the last 30 years for the entire future period (Wanders et al., 2014). Changes in the  $VTM_t$  will also indicate changes in the low flow regime in the 21st century. This approach is different from the more traditional non-transient threshold that is calculated from a control period and that will not adapt to changes in the hydrological regime. Fig. 1 indicates, in a theoretical example, the difference between the traditional non-transient threshold and the transient threshold. It shows that the threshold will gradually change, since the  $VTM_t$  was derived from the discharge of the previous 30-year period, instead of a extrapolation of the threshold based on the discharge from a control period.

## 2.4. Assessment of climate and human impact

To assess the impact of climatic changes on hydrological drought characteristics for the 21st century, two periods were compared. The first period runs from 1971 to 2000 (control period, ctrl) and the second period runs from 2070 to 2099 (future period). For both periods a scenario with natural conditions (pristine) was considered to derive hydrological droughts. In this scenario no human impacts were included and only climate change affects the changes in hydrological drought characteristics. To evaluate the impact of climate change, the changes (in percent) in the low flow regime have been calculated by:

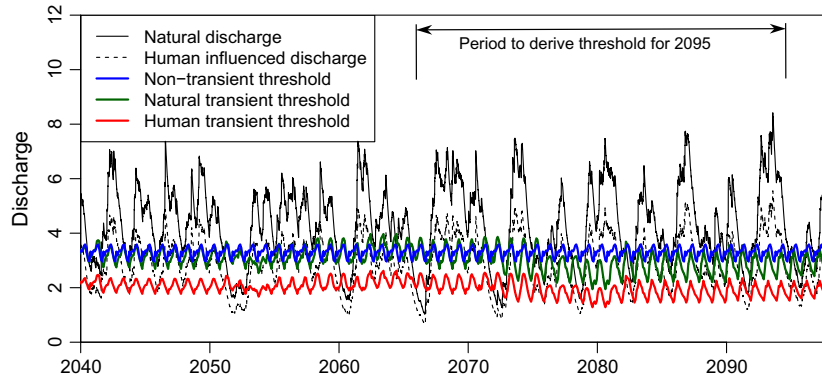


**Fig. 1.** Example time series of threshold calculation for different scenarios. The traditional non-transient threshold is derived from the natural discharge for a control period (typically 1970–2000). The natural transient threshold is derived from the natural discharge of the previous 30-year period. The human transient threshold is derived from the human influenced discharge of the previous 30-year period.

$$dVTM_{clim_t} = \frac{VTM_{future_t} - VTM_{ctrl_t}}{VTM_{ctrl_t}} \times 100 \quad (6)$$

where  $dVTM_{clim_t}$  is the change in the low flow regime,  $VTM_{ctrl_t}$  and  $VTM_{future_t}$  are the transient variable thresholds for the control and future period, respectively. Thereafter, the  $VTM_t$  was used to calculate the drought characteristics, for both the periods. The changes for the future period in the ensuing deficit volumes calculated compared to control period is thus an indication of the impact of climate change on hydrological drought. The relative climate impact on the deficit volume is given by:

$$dDef_{clim} = \frac{Def_{future} - Def_{ctrl}}{Def_{ctrl}} \times 100 \quad (7)$$

where  $dDef_{clim}$  is the relative impact of climate change on the drought deficit volume,  $Def_{ctrl}$  and  $Def_{future}$  are the drought deficit volumes for the control and future period under the pristine condition, respectively.

To assess the impact of human water use and reservoirs on projected changes in hydrological drought characteristics for the 21st century, two scenarios have been used. The pristine scenario has been compared to a scenario with human influences (human). In the scenario with human influences, water is abstracted according to the local water demand and associated reservoir operations are included (Wada et al., 2014). Reservoirs are located on the drainage or river network based on the newly available and extensive Global Reservoir and Dams Dataset (GRaND, Lehner et al., May 2011) that contains 6862 reservoirs with a total storage capacity of 6197 km<sup>3</sup>. The reservoirs were placed over the river network based on the year of their construction. Water is abstracted from surface water (river discharge, reservoirs and lakes) and groundwater, part of it comes back to the river network as return flow and part of it is consumed. Human water use was calculated for the irrigation sector only, since comprehensive sets of socio-economic projections are not yet available consistently across all RCPs under SSPs (Shared Socioeconomic Pathways), which can be used to estimate industrial and domestic water use. Irrigation water use was simulated with PCR-GLOBWB per unit crop area based on the surface water balance (surface water layer for paddy rice) and the soil water balance (soil moisture deficit in the root zone calculated from the difference between the water content at field capacity and the water content at wilting point) (Wada et al., 2014). Irrigated areas were obtained from the MIRCA2000 data set (Portmann et al., 2010). The losses during water transport and irrigation application were included in the calculation based on daily evaporative and percolation losses per unit crop area. Current land use and population density are constant over time since only limited sets

of socio-economic data and no future irrigated area projections are available for the 21st century. Meteorological forcing from five different GCMs with four RCPs have been used to project discharge for the 21st century for both the pristine and human scenario. Effects on projected discharge have been studied, where the changes per RCP were calculated using the ensemble mean of all GCMs. Thereafter, the relative impact of each scenario on the projected changes in hydrological drought has been studied by comparing both scenarios.

For both scenarios the transient threshold ( $VTM_t$ ) was calculated and compared (see Fig. 1 for the example). By making a comparison between both thresholds (one for each scenario), the impact of human water use and reservoirs on the low flow regime can be studied. Additionally, this enables a comparison between the impact of climate change and human water abstraction on the changes in the low flow regime. The impact (in percent) of human influence on the low flow regime is calculated by:

$$dVTM_{human_t} = \frac{HumanVTM_t - PrisVTM_t}{PrisVTM_t} \times 100 \quad (8)$$

where  $dVTM_{human_t}$  is the change in the low flow regime,  $PrisVTM_t$  and  $HumanVTM_t$  are the transient variable thresholds for the pristine and human scenario, respectively. Thereafter, the  $VTM_t$  of the pristine scenario was used to calculate the drought characteristics, for both the pristine and human scenario. By selecting the pristine  $VTM_t$  the relative impact of human influences could be calculated and compared to the impact of climate change. The increase in the ensuing deficit volumes calculated compared to the pristine condition is thus an indication of the anthropogenic intensification of hydrological drought. The relative impact (in percent) of human water abstraction and reservoirs on the deficit volume is given by:

$$dDef_{human} = \frac{HumanDef - PrisDef}{PrisDef} \times 100 \quad (9)$$

where  $dDef_{human}$  is the relative impact of humans on the drought deficit volume,  $HumanDef$  and  $PrisDef$  are the drought deficit volumes under the human and pristine scenario, respectively.

The combined impact of both climate change, and human water use and reservoirs has been studied, by comparing the control period for the pristine scenario with the future period of the human scenario. The relative total impact (in percent) on the deficit volume is given by:

$$dDef_{combi} = \frac{HumanDef_{future} - PrisDef_{ctrl}}{PrisDef_{ctrl}} \times 100 \quad (10)$$

where  $dDef_{combi}$  is the relative combined impact of climate change, and human water use and reservoirs on the drought deficit volume,

$PrisDef_{ctrl}$  is the deficit volume for the control period under pristine conditions and  $HumanDef_{future}$  is the drought deficit volumes for the future period under the human scenario.

In the following sections, the results are presented first on a global scale to assess the regions in which humans have a larger impact than climate on future hydrological drought. Thereafter, the differences between the scenarios were studied for major river basins of the world, where drought events are known to be influenced by human water abstraction and reservoirs regulations (Wada et al., 2013). This would give an improved insight in the hydrological processes and the impact of humans on a river basins scale. Drought characteristics were calculated for the last 30 years of the 21st century for the major river basins.

### 3. Results

#### 3.1. Climate impact on a global scale

On a global scale the impact of climate change on the low flow regime ( $dVTM_{clim_t}$ , Eq. 6) has been evaluated and compared for the control and the future period (Fig. 2). It is shown that climate change has a negative impact on the low flow regime (decrease of 10% or more) in South-America, Australia, Southern-Africa, Southeast Asia and the Mediterranean. Positive impacts on the low flow regime are found in Northwest Africa and large parts of Northern Europe, Russia and Canada. Differences between RCPs are small, whereas a slightly larger impact is found for the higher CO<sub>2</sub> emission scenarios (e.g., RCP6.0 and 8.5).

The impact of climate change on the drought deficit volumes ( $dDef_{clim}$ , Eq. 7) is projected to be severe in large parts of the world (Fig. 3). This is especially true for regions in Northern Africa, Eastern part of the United States and Southern Europe. In these regions drought deficit will likely increase by more than 50%, and for some regions it will increase even up to over 100%. A slightly negative impact (about 10%) exists on the  $dVTM_{clim_t}$  for regions in Southeast Asia and South-America, however, this does not result in a negative impact on the  $dDef_{clim}$ . The agreement amongst different

RCP scenarios is high, and only small uncertainty remains in the projections for North-America and Europe.

It is concluded that the impact of climate change on hydrological drought characteristics is high and associated uncertainties amongst RCPs are low. Although some regions show a negative impact in the low flow regime, this does not necessarily result in increased drought deficit volumes. Overall, drought conditions in most of the world are projected to be negatively impacted by climatic changes.

#### 3.2. Impact of human water use on a global scale

On a global scale the thresholds for the pristine scenario and the human scenario ( $dVTM_{human_t}$ , Eq. 8) have been compared (Fig. 4). As expected the  $dVTM_{human_t}$  decreased in Asia and the Mediterranean, where the impact of human water use exceeds the compensating effect brought by reservoirs operations. The water abstraction in these regions results in a negative impact on the low flow regime, where low flows reduce as a result of the water abstraction. For central Europe and the United States the reservoir regulation measures compensate the negative impact caused by water abstraction and overall human influences have a positive impact on the low flows. Similar to the climate change impacts, differences between different RCP scenarios are small, with only slightly higher  $dVTM_{human_t}$  values for RCP2.6. This is likely caused by the relatively small impact of the climate on  $dVTM_{human_t}$  compared to that of human water abstraction. For RCP8.5 the impact of climate change is project to be more severe compared to the human contribution to the overall changes in the low flow regime.

The impact of humans on the drought deficit volumes ( $dDef_{human}$ , Eq. 9) is more pronounced than the impact on the  $dVTM_{human_t}$  (Fig. 5), which is mainly caused by the reduced water availability as a result of water use. In some regions abstractions and water regulation measures account for almost 200% of the net increase in deficit volume for the 21st century. A negative  $dDef_{human}$  is found where water regulating measures reduce drought deficits as a direct result of water retention over the year.

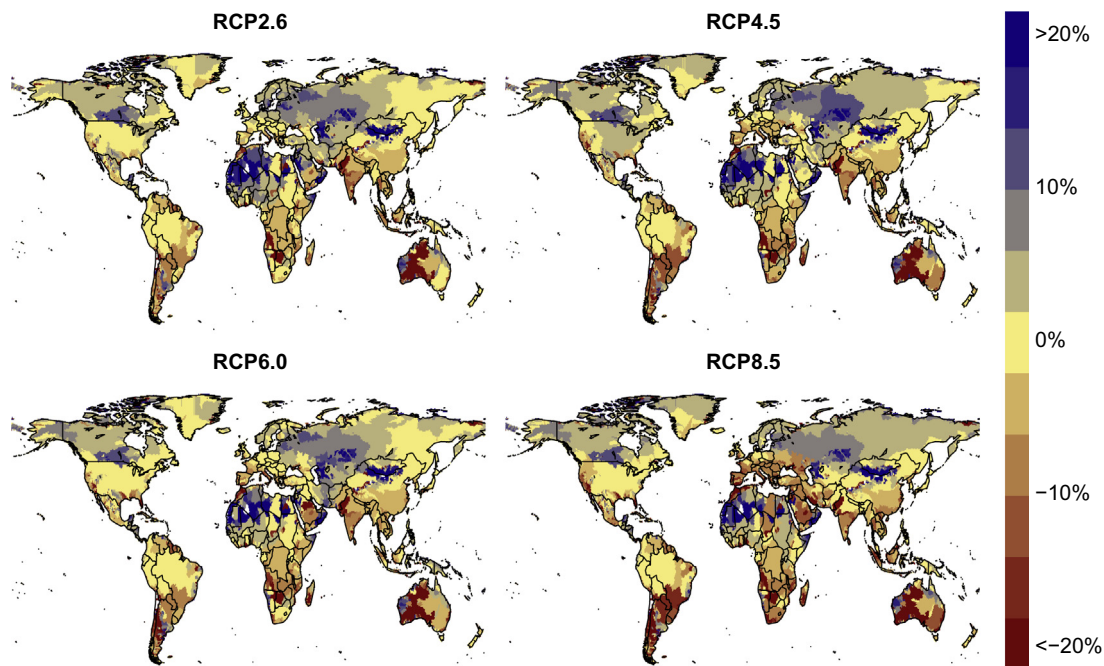
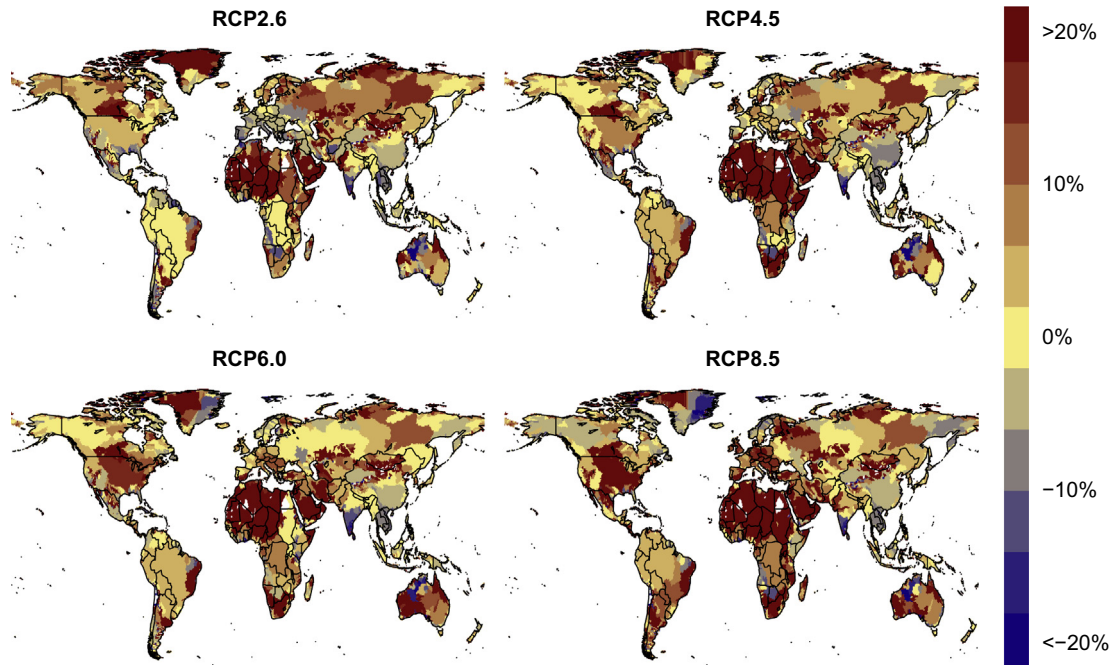
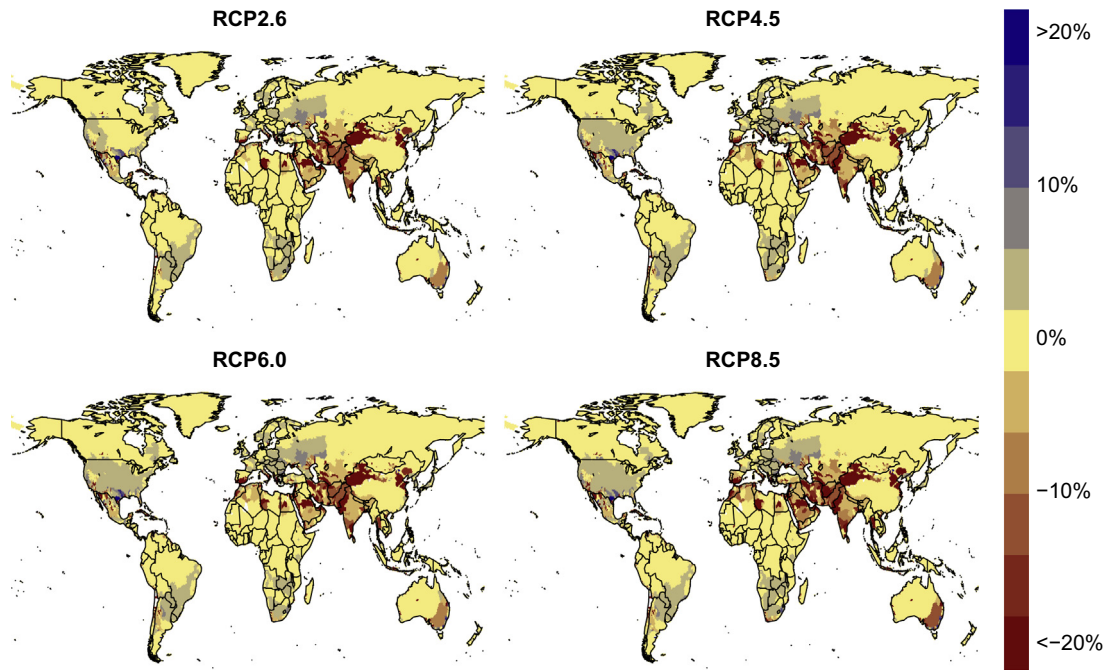


Fig. 2. Climate impact on drought threshold ( $Q_{90}$ ,  $dVTM_t$ ) compared between the periods 1971–2000 and 2070–2099. Impact is calculated as a percent where positive percentages indicate an increase in the  $Q_{90}$  and negative percentages indicate a decrease in the  $Q_{90}$  as a result of climate change. Each plot gives the ensemble mean impact derived from 5 GCMs for different RCPs.



**Fig. 3.** Climate impact on drought deficit volume ( $dDef$ ), compared between the periods 1971–2000 and 2070–2099. Each plot gives the annual average impact derived from 5 GCMs for different RCP scenarios. Impact is calculated as a percent, where positive percentages indicate a increase in the drought deficit volume and negative percentages indicate a decrease in the drought deficit volume as a result of climate change.



**Fig. 4.** Impact of reservoirs and human water use on drought threshold ( $Q_{90}$ ) compared to the pristine conditions ( $dVTM_{human,t}$ ), over the period 2070–2099. Impact is calculated as a percent where positive percentages indicate an increase in the  $Q_{90}$  and negative percentages indicate a decrease in the  $Q_{90}$  as a result of human water use and reservoirs. Each plot gives the ensemble mean impact derived from 5 GCMs for different RCPs.

This effect is found in large parts of Europe, where a large number of reservoirs exist. Additionally, regions in Southern Africa and South America show a impact of the reservoirs operations on the drought deficit volumes. Differences between RCPs are minor indicating that the contribution of humans to the changes in drought deficit is proportional to the changes in the climate. From this analysis it was derived that the mechanisms between drought, and human water use and reservoir regulation measures is nontrivial.

The combined effect of human water use and river regulations could result in both a positive or negative impact on the low flow regime.

### 3.3. Combined impact on a global scale

The impact of climate change, and human water use and reservoirs has been studied for the changes in deficit volumes ( $dDef_{combi}$ ,

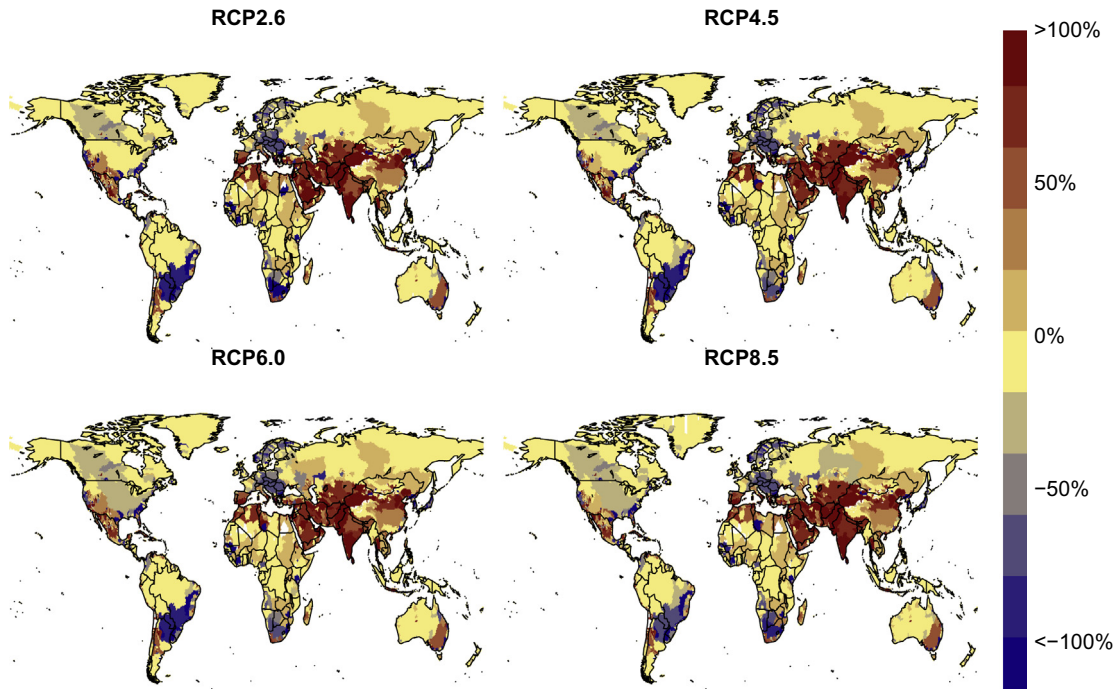


**Fig. 5.** Impact of reservoirs and human water use on drought deficit volume compared to the pristine conditions ( $dDef_{human}$ ), over the period 2070–2099. Each plot gives the annual average impact derived from 5 GCMs for different RCP scenarios. Impact is calculated as a percent, where positive percentages indicate an increase in the drought deficit volume and negative percentages indicate a decrease in the drought deficit volume as a result of human water use and reservoirs.

Eq. 10). To this end, the pristine scenario under the control period was compared to the human scenario under the future period (i.e., the end of this century, Fig. 6). It is clear that the combined impact results in severely increased drought deficit volumes, up to 100% from the control period. Regions include Southeast Asia and the Mediterranean, which are not projected to be impacted by climate

change (Fig. 3), will likely be heavily impacted by the additional driving force of the human water use. The severity of the  $dDef_{combi}$  increase is less severe for regions in Russia, Europe and North-America. Although different RCP scenarios agree upon to a high degree, for Europe the directionality of the changes is expected to be dependent on the RCP. It is concluded that the com-

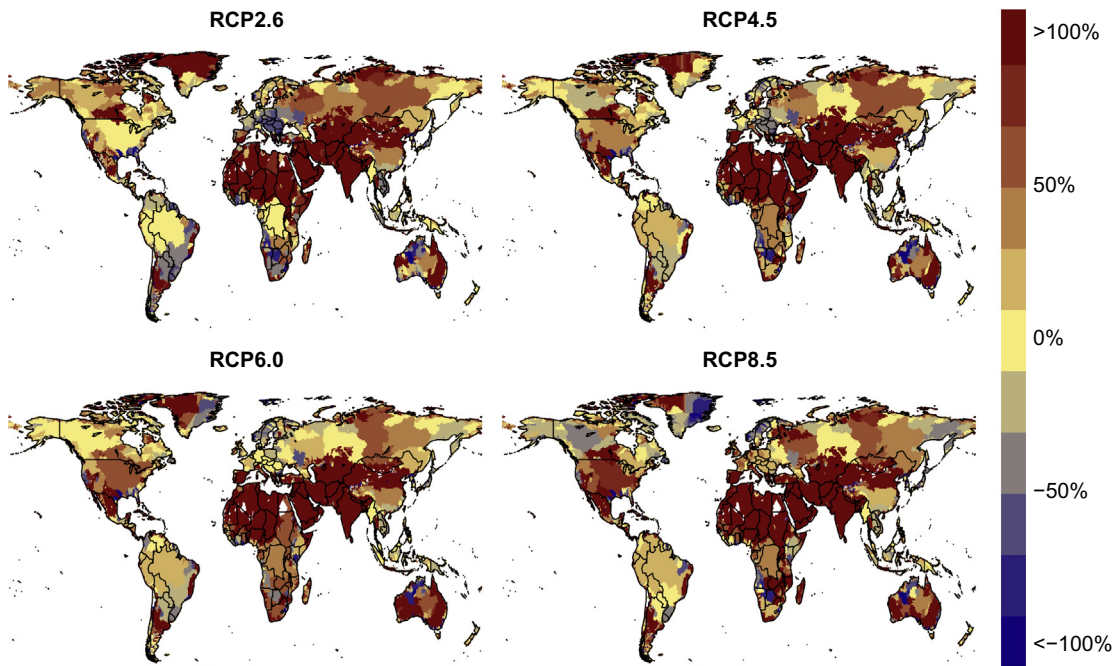


**Fig. 6.** Impact of climate change, human water use and reservoirs on drought deficit volume ( $dDef_{combi}$ ), comparison between the periods 1971–2000 (pristine scenario) and 2070–2099 (water use scenario). Each plot gives the annual average impact derived from 5 GCMs for different RCP scenarios. Impact is calculated as a percent, where positive percentages indicate an increase in the drought deficit volume and negative percentages indicate a decrease in the drought deficit volume as a result of climate change, human water use and reservoirs.

combined impact overall results in an increased drought deficit volumes and hence increases drought vulnerability, especially for Southeast Asia, Middle East and North-Africa.

#### 3.4. Impact of climate and human water use – seasonal decomposition

The impacts of climate change, and reservoirs and human water use on the drought deficit have been studied for each season separately. To assess the impact of climate change the control and future period under the pristine scenario were compared (Fig. 7) while for the impact of human water use and reservoirs the human and pristine scenario have been compared, for the period 2070–2099 (Fig. 8). For these analyses, the simulations for all RCPs were averaged, because it was shown by our previous analyses (see Figs. 2–5) that the differences between RCPs are minor.

The impact of climate change is visible throughout the world (Fig. 7), where the largest impacts are again found in Northern Africa, Eastern part of the United States and Southern Europe. Seasonality in the projected changes is mainly found in Europe and North-America, where the biggest increase in drought deficit volumes is found in winter (December–January–February). In the other seasons the impact of climate change is projected to be less or even reduce the observed drought deficit volumes. A non-seasonal or constant climate impact is found for Northern-Africa (negative) and Southeast Asia (positive).

Clear patterns are also visible for the impact of human water use and reservoirs, for example in Asia and the Mediterranean, again, showing a positive  $dDef_{human}$  (Fig. 8). The magnitude of the  $dDef_{human}$  varies over the year, with a peak in the respective dry season for each region. For the United States, spring droughts are projected to be more severe as a result of water retention of the snow melt peak in reservoirs. Drought deficit volumes in summer and autumn for the United States are projected to decrease as a result of increased water compared to the pristine conditions. In Europe, reservoirs result in a longer retention of water throughout the year, leading to less seasonal discharge and hence lower deficit volumes.

#### 3.5. River discharge simulation and impact of human water use per basin

For selected river basins (e.g. Mississippi and Indus) the discharge between the pristine and human scenario has been compared, to study the impact of reservoirs and human water use on the discharge regime (Figs. 9 and 10). As expected, annual discharge decreased as a result of increased evapotranspiration due to irrigation water use. However, the addition of reservoirs to the river network has a dampening impact on the annual cycle in the discharge regime. Although, annual average discharge generally decreased as a result of increased evapotranspiration from the water surface of the reservoirs and irrigation, the decrease is not equally distributed throughout the year. In general, peak flows are reduced as a result of the buffering capacity of the reservoirs and low flow levels are increased even though the water abstraction results in overall lower water availability. The dampening effect for some rivers is projected to result in a decreased drought severity in the low flow season due to increased water availability. This effect is obvious in some, mostly strongly regulated, river basins in the world where human water abstraction does not exceed the compensating effect (i.e., buffering capacity) of the reservoirs on the low flows. These river basins are mainly situated in Europe and North America (e.g. Mississippi, Fig. 9). The dampening effect is mainly important in the low flow season when discharge rates are low and droughts tend to have the largest impact on the natural ecosystem and society.

Other major river basins suffer from large abstractions of water for irrigation, resulting in an overall decreased water availability throughout the year. For these basins, the reservoir regulating measures are not enough to compensate the abstraction, and thus the low flow regime changes to even drier conditions. This effect is especially strong for some major river basins in the Middle East and Asia (e.g. Indus, Fig. 10). In these regions, human water abstractions are large and have a strong negative impact on the drought severity and vulnerability. The projected impacts vary slightly for different RCPs, however, the trend directions are simi-

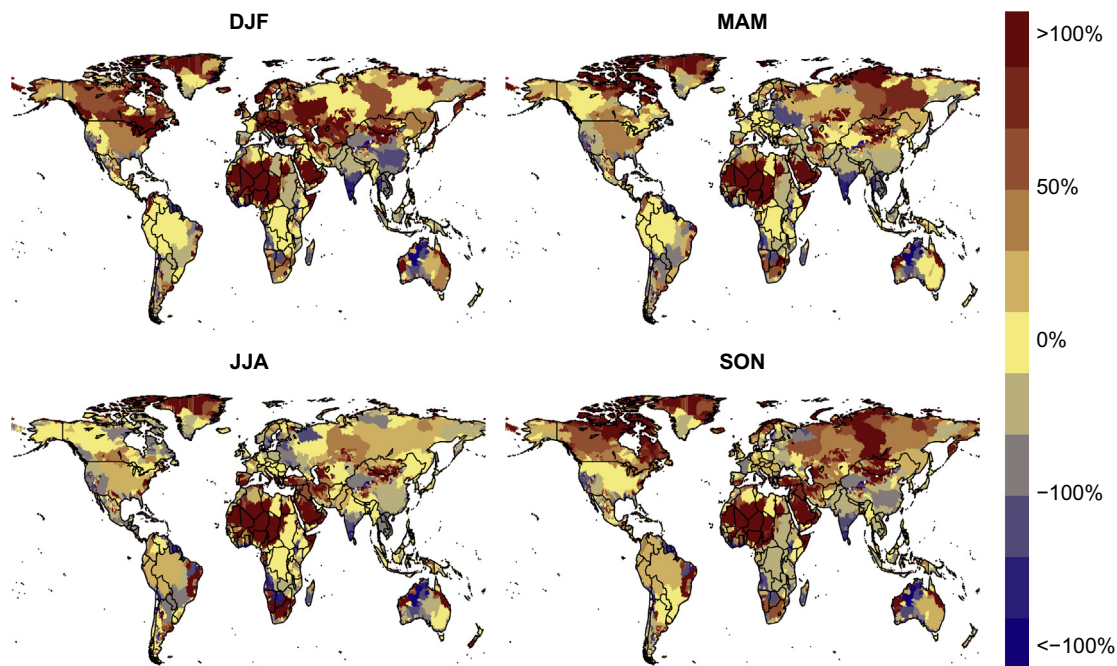


**Fig. 7.** Impact of climate change on drought deficit volume ( $dDef$ ) comparison between the periods 1971–2000 and 2070–2099. Each plot gives the seasonal average derived from 5 GCMs and 4 RCPs. Impact is calculated as a percent, where positive percentages indicate an increase in the drought deficit volume and negative percentages indicate a decrease in the drought deficit volume as a result of climate change.

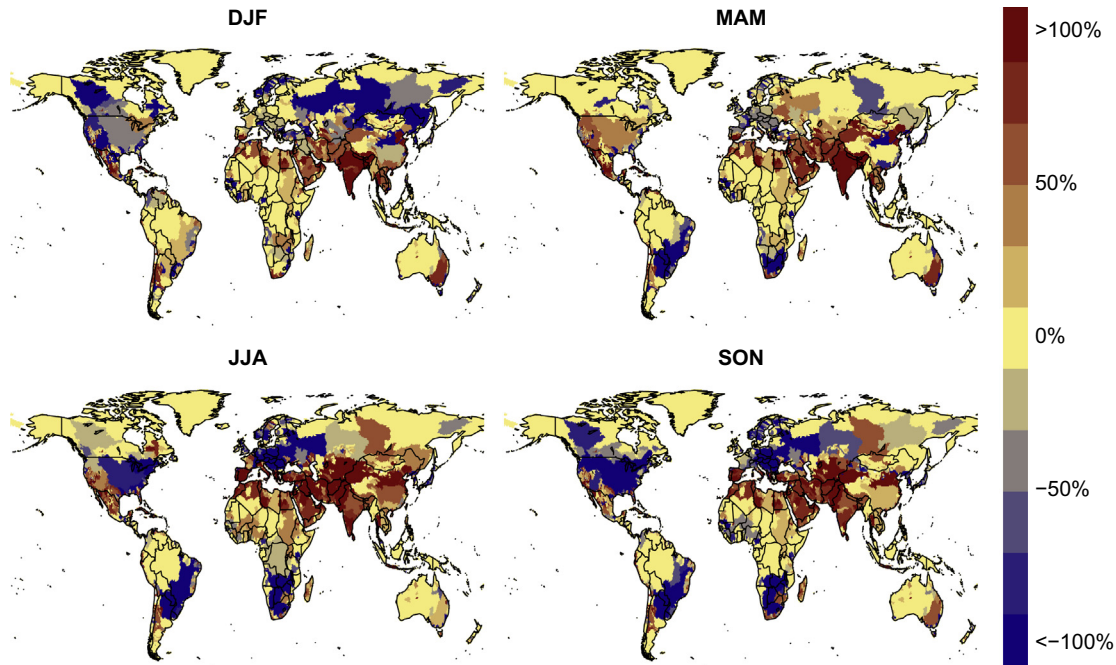


**Fig. 8.** Impact of reservoirs and human water use on drought deficit volume compared to the pristine conditions ( $dDef_{human}$ ) per season, over the period 2070–2099. Each plot gives the seasonal average derived from 5 GCMs and 4 RCPs. Impact is calculated as a percentage, where positive percentages indicate an increase in the drought deficit volume and negative percentages indicate a decrease in the drought deficit volume as a result of human water use and reservoirs.

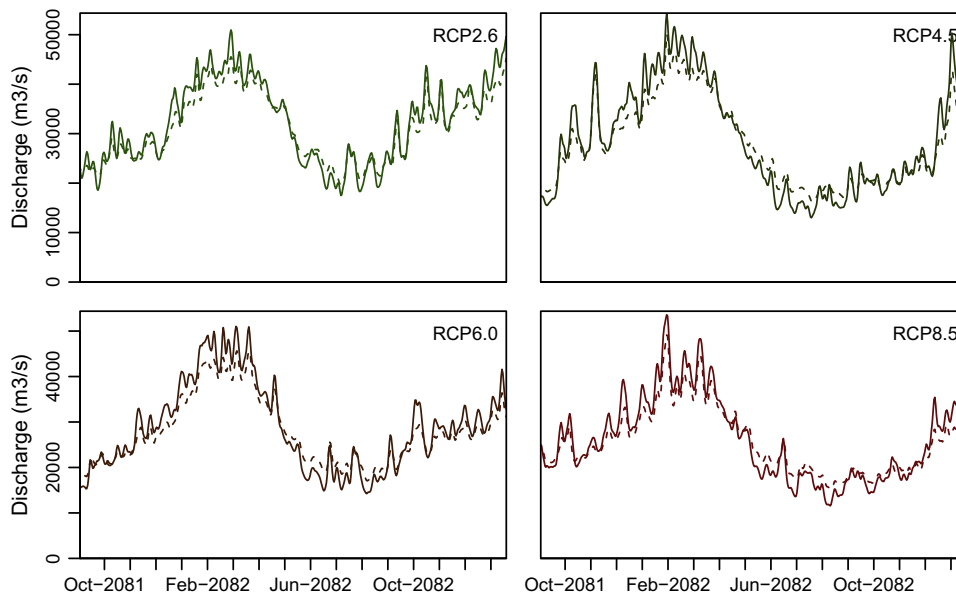


**Fig. 9.** Average discharge over 5 GCMs per RCP for the Mississippi river. Solid line indicates the natural scenario without human water abstractions and reservoirs, and the dashed line gives the river discharge under human influences.

lar. For the Mississippi (Fig. 9) a regime shift with earlier peak flows is projected for the RCPs with a higher temperature rise (RCP6.0 and 8.5), leading to increased and earlier snowmelt. This also impacts the timing and level of the low flow regime. For the Indus (Fig. 10) the water availability is projected to increase from RCP2.6 to RCP8.5. However, the water abstraction is also projected to increase towards RCP8.5 leading to a significant reduction of the low flow level.

The changes in the streamflow climatology show a decrease in total water availability for the selection of the major river basins (Fig. 11). On average the streamflow climatology will likely be smoothed throughout the year due to reservoir regulation. The

combined impact of this reduced water availability and regulation measures does not always result in a reduction of the threshold as is shown in Fig. 12. The threshold under human influence is not always lower than the pristine threshold (e.g. Mississippi, Colorado, Volga) and the regulation measures counteract the reduced water availability.

Drought characteristics have been calculated to analyse the impact of reservoirs and human water use on the severity and frequency of drought events (Tables 3 and 4) for selected river basins. In the current situation (1971–2000) the drought frequency, severity and intensity are increased due to human influences for almost all rivers. The human impact is very large in regions known to be

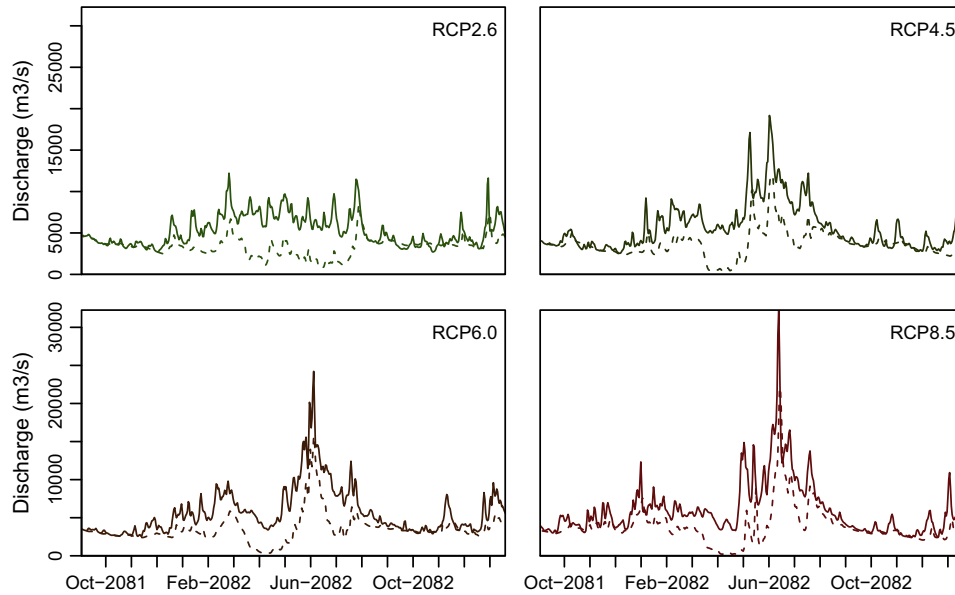


**Fig. 10.** Average discharge over 5 GCMs per RCP for the Indus river. Solid line indicates the natural scenario without human water abstractions and reservoirs, and the dashed line gives the river discharge under human influences.

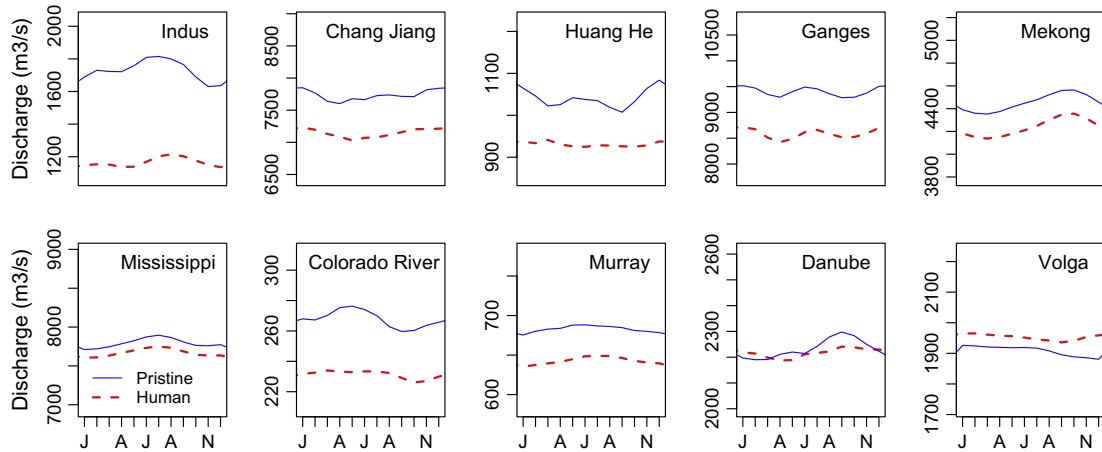


**Fig. 11.** Average discharge climatology derived from 5 GCMs and 4 RCPs for 10 selected river basins, for the period 2070–2099. The pristine scenario (blue) and scenario with human influences (red) are given. (For interpretation of the references to colour in this figure legend, the reader is referred to the web version of this article.)

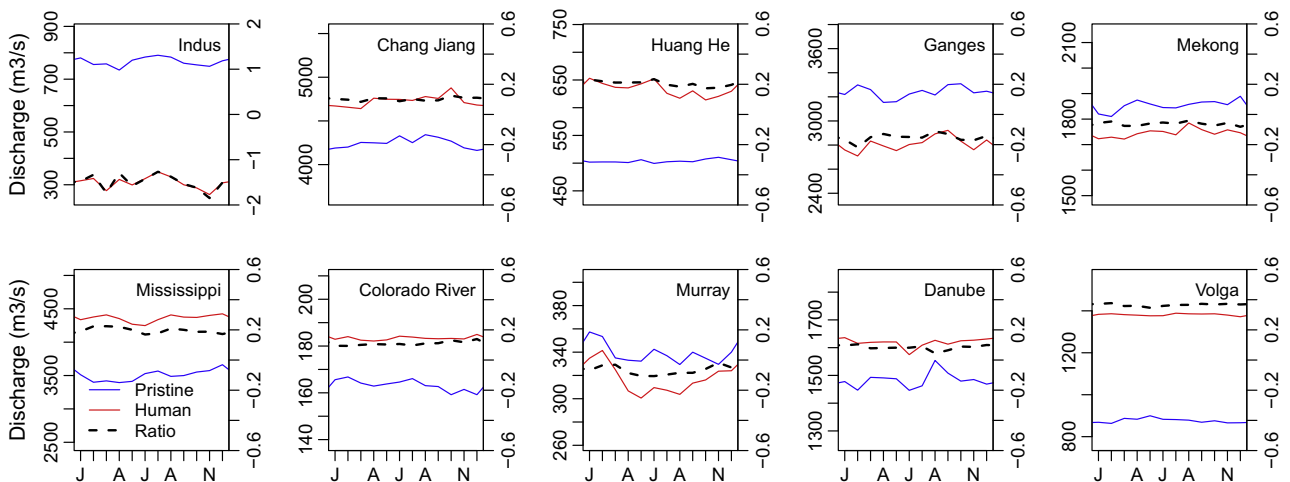


**Fig. 12.** Average low flow regime (i.e. thresholds) derived from 5 GCMs and 4 RCPs for 10 selected river basins, for the period 2070–2099. Solid lines indicate the pristine (blue) and water demand (red) scenarios, dashed line gives the fractional difference between the two low flow climatologies (with pristine as reference). In other words the dashed lines show the fractional change in the low flow regime as a result of reservoirs and human water abstractions, where a positive ratio indicates increased the low flow regime. (For interpretation of the references to colour in this figure legend, the reader is referred to the web version of this article.)

**Table 3**  
Impact of reservoirs and human water abstractions on drought characteristics compared to the pristine conditions, for the period 1971–2000 and selected rivers. Average drought duration, deficit volume per drought event and the total drought intensity are given. The drought characteristics are obtained with the pristine threshold (derived from the period 1971–2000). The characteristics are averaged over all RCPs and GCMs.

River	Pristine			Human		
	Average event		Drought	Average event		Drought
	Duration (d)	Deficit ( $\text{m}^3 \text{s}^{-1}$ )	Intensity ( $\text{m}^3 \text{s}^{-1} \text{d}^{-1}$ )	Duration (d)	Deficit ( $\text{m}^3 \text{s}^{-1}$ )	Intensity ( $\text{m}^3 \text{s}^{-1} \text{d}^{-1}$ )
Indus	6.68	3642	545	32.59	67098	2059
Yangtze	5.68	9324	1640	10.36	32223	3110
Huang He	3.42	449	131	32.26	43753	1356
Ganges	4.57	5973	1306	10.92	22438	2054
Mekong	12.96	9344	721	21.72	21504	990
Mississippi	12.71	36501	2873	16.47	43569	2645
Colorado	5.26	494	94	26.83	5452	203
Murray-Darling	29.69	11934	402	37.81	17409	460
Danube	8.48	7581	893	13.88	10549	760
Volga	11.67	7179	615	25.66	46129	1797

**Table 4**  
Impact of reservoirs and human water abstractions on drought characteristics compared to the pristine conditions, for the period 2070–2099 and selected rivers. Average drought duration, deficit volume per drought event and the total drought intensity are given. The drought characteristics are obtained with the transient pristine threshold (derived from the period 30-year moving window). The characteristics are averaged over all RCPs and GCMs.

River	Pristine			Human		
	Average event		Drought	Average event		Drought
	Duration (d)	Deficit ( $\text{m}^3 \text{s}^{-1}$ )	Intensity ( $\text{m}^3 \text{s}^{-1} \text{d}^{-1}$ )	Duration (d)	Deficit ( $\text{m}^3 \text{s}^{-1}$ )	Intensity ( $\text{m}^3 \text{s}^{-1} \text{d}^{-1}$ )
Indus	7.75	4866	628	33.65	70173	2085
Yangtze	6.58	11481	1744	10.51	33011	3142
Huang He	4.27	535	125	28.84	37828	1312
Ganges	4.07	4507	1107	13.00	24083	1852
Mekong	15.60	11601	743	27.50	31481	1145
Mississippi	15.68	50522	3221	17.91	50342	2810
Colorado	6.21	691	111	25.56	4855	190
Murray-Darling	38.15	17076	448	52.50	27947	532
Danube	9.31	9324	1002	15.44	13033	844
Volga	11.43	9083	794	24.62	36724	1492

affected by severe water abstractions such as Asia and North America. For example, the Huang He and Colorado are severely impacted and drought characteristics are intensified by five to tenfold compared to the natural conditions. In general, drought events tend to be more severe and frequent for the selected river basins. When the  $VTM_t$  is applied to the future period, drought characteristics in the pristine simulation do not significantly change. However, since the  $VTM_t$  is adapted to the climatology, the actual low flow level might still reduce significantly, as shown in Fig. 12. The human influence on drought shows that the drought intensity increases for all rivers, with the exception of the Mississippi and Danube. In these rivers, the reservoirs result in more regulated discharge leading to longer, but less severe drought events. The increase in deficit volume impacts the severity of the drought events and likely increases the vulnerability of our society and nature. The relative increase in drought deficits is largest for the Indus and Huang He, while for the Mississippi the impacts are minor as a result of strong river regulation measures. It should be noted that for many river basins in the world no impact was found since human water use is negligible and reservoir regulations are minimal or reservoirs are absent. In general, human water use increases drought duration and severity, however, this effect can be (partly) compensated by reservoir regulations that retain the water for prolonged periods.

#### 4. Discussion and conclusions

In this study the impact of climate change, and human water use and reservoirs on projected hydrological drought characteris-

tics for the 21st century has been studied. Obtained future simulation results were compared to the control period or the pristine scenario (climate change only) and the relative contribution of humans was compared to the impact of climate change. The impact of climate change on the low flow regime and hydrological drought characteristics is projected to be severe. Large regions are expected to suffer from a negative impact of climate change on drought deficit volumes. Additionally, it was found that the impact of water use and reservoir on hydrological drought characteristics is none trivial and can vary depending on the local climate and available water resources.

The approach used here is limited by the analysis of only one GHM, where it would be more comprehensive to use an ensemble of GHMs (e.g. Prudhomme et al., 2014; Van Huijgevoort et al., 2014). However, due to the fact that many GHMs do not incorporate the human water abstraction or reservoir regulations, this type of analysis is difficult. Nevertheless, a multi GHM analysis would increase our understanding of uncertainties in future projections of the impact of humans on hydrological drought.

A limitation of the present study is that the abstraction of water is related to the current extent of agricultural irrigation for each region. The expected expansion of irrigated areas is projected to cause a further increase in irrigation water demand in some regions (e.g., Africa, South America). Additionally, population growth will result in increased demand for drinking water and industrial activities (Wada et al., 2013), leading to a higher water demand. Especially in areas like Africa, the population is projected to increase substantially. The changes in land use could also significantly alter the propagation of drought and hydrological drought characteristics (Van Lanen et al., 2013). The projected changes in

population and land use were currently not included, due to low data availability and high projection uncertainty, but could be important when higher accuracy is warranted for future projections. Future hydrological drought characteristics may be altered for regions like Africa, where changes are expected, in both water demand and land use.

Since the relative contribution of human influence on hydrological drought for the 21st century has not been studied globally to our knowledge, it is difficult to compare the obtained results with existing studies. However, areas with a high human impact on drought characteristics as identified in this study have been also indicated by Wada et al. (2014) showing high groundwater depletion rates. One of the main conclusions from this study is that the increased drought vulnerability as a direct result of human water abstraction can be compensated by river regulating measure of reservoirs. Reservoirs retain the water for longer times compared to pristine conditions and thus lead to a smoothed hydrograph, with lower peak flows and higher low flows. This will also directly impact the severity of droughts in the human-controlled systems, where the low flows are partly compensated by extra water availability due to retention in the reservoirs. This phenomenon is mainly found in the United States and Europe, where the number of reservoirs is large.

Furthermore, it is found that human influence can account for almost 100% of the changes in future hydrological drought in areas such as Asia, Middle East and the Mediterranean. These areas are heavily impacted by water abstraction and reservoirs are not enough to compensate for these severe water abstractions. In these regions low flows are expected to be even lower in future and drought deficit volumes will likely increase significantly. The differences among the RCPs in the obtained results are minor, indicating that the impact of human influence is proportional to the magnitude of the climate change.

Finally, the seasonal changes in drought characteristics were studied by looking at the projected drought events for the period 2070–2099 and the relative contribution of climate change and humans to these events. Climate change is projected to result in increased deficit volumes in large parts of the world, however, seasonal effects play an important role. The impact of summer drought in the Northern Hemisphere is expected to be lower or sometimes result in decreased drought deficit volumes. It is shown that reservoirs increase the drought deficit volumes in the wet season, when the water availability is high, and reduces the deficit volume in the dry season. In the dry season the retained water in the reservoirs is slowly released, positively impacting deficit volumes compared to the pristine scenario. In large parts of Asia, the Middle East and the Mediterranean a high impact of human water abstraction on future drought deficits is found. The impact varies throughout the year and shows a high correlation with the temporal pattern in human water demand. In the crop growing season, water abstractions are project to be more severe leading to more severe drought events, while the impact is expected to be reduced in the wet season, due to large water availability and lower human water demands.

It is concluded that the human impact on projected hydrological drought is pronounced, which has been neglected in most projections for future hydrological drought. Better scenarios of future human water demand could lead to a more skilful projection for the 21st century, however, they are not available yet due to the lack of comprehensive future socio-economic and land use projections that are consistent with each another. Human water use and reservoirs have nowadays substantial impacts on global hydrology and water resources, and should therefore be included in global hydrological models that are used for projections of the future hydrological droughts. This will significantly improve our understanding of future hydrology and the changes in hydrological drought characteristics.

## Acknowledgments

NW was funded by a grant from the user support program Space Research of NWO (contract number NWO GO-AO/30). This work has been supported by the framework of ISI-MIP funded by the German Federal Ministry of Education and Research (BMBF) (Project funding reference number: 01LS1201A). We thank anonymous reviewers and guest Editor (Ashok Mishra) for their constructive suggestions, which helped to improve the manuscript.

## References

- Alderlieste, M.A.A., Van Lanen, H.A.J., Wanders, N., 2014. Future low flows and hydrological drought: how certain are these for Europe. In: Daniell, T., Van Lanen, H., Demuth, S., Laaha, G., Servat, E., Mahe, G., Boyer, J.-F., Paturel, J.-E., Dezetter, A., Ruelland, D. (Eds.), *Hydrology in a Changing World: Environmental and Human Dimensions*, vol. 363. IAHS Publications, pp. 60–65.
- Andreadis, K.M., Clark, E.A., Wood, A.W., Hamlet, A.F., Lettenmaier, D.P., 2005. Twentieth-century drought in the conterminous united states. *J. Hydrometeorol.* 6 (6), 985–1001.
- Arguez, A., Vose, R.S., 2010. The definition of the standard WMO climate normal: the key to deriving alternative climate normals. *B. Am. Meteorol. Soc.* 92 (6), 699–704.
- Bergström, S., 1995. The HBV model. In: *Computer Models of Watershed Hydrology*. Water Resour. Publ., Highlands Ranch, Colorado, USA.
- Burke, E.J., Brown, S.J., Christidis, N., 2006. Modeling the recent evolution of global drought and projections for the twenty-first century with the Hadley centre climate model. *J. Hydrometeorol.* 7 (5), 1113–1125.
- Corzo-Perez, G.A., Van Lanen, H.A.J., Bertrand, N., Chen, C., Clark, D., Folwell, S., Gosling, S.N., Hanasaki, N., Heinke, J., Vo, F., 2011. Drought at the Global Scale in the 21st Century. Tech. Rep. 43. EU WATCH (Water and global Change) Project <<http://www.eu-watch.org>> (retrieved 01.03.12).
- Dai, A., 2011. Drought under global warming: a review. *Wiley Interdiscipl. Rev.: Clim. Change* 2 (1), 45–65.
- Dai, A., 2013. Increasing drought under global warming in observations and models. *Nature Clim. Change* 3, 52–58.
- Dracup, J., Lee, K., Paulson Jr., E., April 1980. On the definition of droughts. *Water Resour. Res.* 16 (2), 297–302.
- Feyen, L., Dankers, R., 2009. Impact of global warming on streamflow drought in Europe. *J. Geophys. Res.-Space* 114 (D17), D17116.
- Fleig, A., Tallaksen, L., Hisdal, H., Demuth, S., 2006. A global evaluation of streamflow drought characteristics. *Hydrol. Earth Syst. Sci.* 10, 535–552.
- Forzieri, G., Feyen, L., Rojas, R., Flörke, M., Wimmer, F., Bianchi, A., 2014. Ensemble projections of future streamflow droughts in Europe. *Hydrol. Earth Syst. Sci.* 18 (1), 85–108.
- Gleick, P.H., 2000. A look at twenty-first century water resources development. *Water Int.* 25 (1), 127–138.
- Gleick, P.H., 2010. Roadmap for sustainable water resources in southwestern North America. *Proc. Natl. Acad. Sci.* 107 (50), 21300–21305.
- Hagemann, S., Gates, L.D., 2003. Improving a sub-grid runoff parameterization scheme for climate models by the use of high resolution data derived from satellite observations. *Clim. Dynam.* 21, 349–359.
- Hamon, W.R., 1963. Computation of direct runoff amounts from storm rainfall. *IAHS Publ.* 63, 52–62.
- Hempel, S., Frieler, K., Warszawski, L., Schewe, J., Piontek, F., 2013. A trend-preserving bias correction – the ISI-MIP approach. *Earth Syst. Dynam.* 4 (2), 219–236.
- Hisdal, H., Tallaksen, L., Peters, E., Stahl, K., Zaidman, M., 2001. Drought Event Definition. Technical Report No. 6. Tech. Rep. Final Report to the European Union – ARIDE Project.
- Hisdal, H., Tallaksen, L., Clausen, B., Peters, E., Gustard, A., 2004. Hydrological drought characteristics. In: Tallaksen, L., Van Lanen, H. (Eds.), *Hydrological Drought: Processes and Estimation Methods for Streamflow and Groundwater*, Development in Water Science, vol. 48. Elsevier, pp. 139–198.
- Kraijenhof van de Leur, D., 1962. Some effects of the unsaturated zone on nonsteady free-surface groundwater flow as studied in a sealed granular model. *J. Geophys. Res.-Space* 67 (11), 4347–4362.
- Lehner, B., Dll, P., Alcamo, J., Henrichs, T., Kaspar, F., 2006. Estimating the impact of global change on flood and drought risks in Europe: a continental, integrated analysis. *Clim. Change* 75 (3), 273–299.
- Lehner, B., Liermann, C.R., Revenga, C., Vrsnsmarty, C., Fekete, B., Crouzet, P., Dll, P., Endejan, M., Frenken, K., Magome, J., Nilsson, C., Robertson, J.C., Rdel, R., Sindorf, N., Wisser, D., May 2011. High-resolution mapping of the world's reservoirs and dams for sustainable river-flow management. *Front. Ecol. Environ.* 9 (9), 494–502.
- Mishra, A.K., Singh, V.P., 2010. A review of drought concepts. *J. Hydrol.* 391 (1–2), 202–216.
- Parry, S., Prudhomme, C., Hannaford, J., Lloyd-Hughes, B., 2010. Examining the spatio-temporal evolution and characteristics of large-scale European droughts. In: Kirby, C. (Ed.), *Role of Hydrology in Managing Consequences of a Changing Global Environment*. Proceedings of the BHS Third International Symposium. British Hydrological Society, pp. 135–142.

- Pederson, N., Bell, A.R., Knight, T.A., Leland, C., Malcomb, N., Anchukaitis, K.J., Tackett, K., Scheff, J., Brice, A., Catron, B., Blozan, W., Riddle, J., 2012. A long-term perspective on a modern drought in the American southeast. *Environ. Res. Lett.* 7 (1), 014034.
- Portmann, F., Siebert, S., Döll, P., 2010. Mirca 2000 – global monthly irrigated and rainfed crop areas around the year 2000: a new high-resolution data set for agricultural and hydrological modeling. *Global Biogeochem. Cyc.* 24 (1), GB1011.
- Prudhomme, C., Giuntoli, I., Robinson, E.L., Clark, D.B., Arnell, N.W., Dankers, R., Fekete, B.M., Franssen, W., Gerten, D., Gosling, S.N., Hagemann, S., Hannah, D.M., Kim, H., Masaki, Y., Satoh, Y., Stacke, T., Wada, Y., Wisser, D., 2014. Hydrological droughts in the 21st century, hotspots and uncertainties from a global multimodel ensemble experiment. *Proc. Natl. Acad. Sci.* 111 (9), 3262–3267.
- Seager, R., 2007. The turn of the century North American drought: global context, dynamics, and past analogs. *J. Climate* 20 (22), 5527–5552.
- Sheffield, J., Wood, F., 2007. Characteristics of global and regional drought, 1950–2000: analysis of soil moisture data from off-line simulation of the terrestrial hydrologic cycle. *J. Geophys. Res.-Space* 112, D17115.
- Sheffield, J., Wood, E.F., Roderick, M.L., 2012. Little change in global drought over the past 60 years. *Nature* 491 (7424), 435–438.
- Sutanudjaja, E.H., van Beek, L.P.H., de Jong, S.M., van Geer, F.C., Bierkens, M.F.P., 2014. Calibrating a large-extent high-resolution coupled groundwater-land surface model using soil moisture and discharge data. *Water Resour. Res.* 50, 687–705.
- Tallaksen, L.M., Madsen, H., Clausen, B., 1997. On the definition and modelling of streamflow drought duration and deficit volume. *Hydrol. Sci.* 42 (1), 15–33.
- Tallaksen, L.M., Hisdal, H., van Lanen, H.A.J., 2009. Space-time modelling of catchment scale drought characteristics. *J. Hydrol.* 375, 363–372.
- Trenberth, K.E., Branstator, G.W., Arkin, P.A., 1988. Origins of the 1988 North American drought. *Int. Sci. Technol. Pol. Inn.* 242 (4886), 1640–1645.
- Trenberth, K.E., Dai, A., van der Schrier, G., Jones, P.D., Barichivich, J., Briffa, K.R., Sheffield, J., 2014. Global warming and changes in drought. *Nature Clim. Change* 4 (1), 17–22.
- Van Beek, L.P.H., Wada, Y., Bierkens, M.F.P., 2011. Global monthly water stress: I. Water balance and water availability. *Water Resour. Res.* 47, W07517.
- Van Huijgevoort, M.H.J., Hazenberg, P., Van Lanen, H.A.J., Uijlenhoet, R., 2012. A generic method for hydrological drought identification across different climate regions. *Hydrol. Earth Syst. Sci.* 16 (8), 2437–2451.
- Van Huijgevoort, M.H.J., Van Lanen, H.A.J., Teuling, A.J., Uijlenhoet, R., 2014. Identification of changes in hydrological drought characteristics from a multi-gcm driven ensemble constrained by observed discharge. *J. Hydrol.* 512, 421–434.
- Van Huijgevoort, M.H.J., Hazenberg, P., van Lanen, H.A.J., Teuling, A.J., Clark, D.B., Folwell, S., Gosling, S.N., Hanasaki, N., Heinke, J., Koirala, S., Stacke, T., Voss, F., Sheffield, J., Uijlenhoet, R., Jul, 2013. Global multimodel analysis of drought in runoff for the second half of the twentieth century. *J. Hydrometeorol.* 14 (5), 1535–1552.
- Van Lanen, H.A.J., Wanders, N., Tallaksen, L.M., Van Loon, A.F., 2013. Hydrological drought across the world: impact of climate and physical catchment structure. *Hydrol. Earth Syst. Sci.* 17 (5), 1715–1732.
- Van Loon, A.F., Tijdeman, E., Wanders, N., Van Lanen, H.A.J., Teuling, A.J., Uijlenhoet, R., 2014. How climate seasonality modifies drought duration and deficit. *J. Geophys. Res.: Atmos.* 119, 4640–4656.
- Van Vuuren, P., Edmonds, J., Kainuma, M., Riahi, K., Thomson, A., Hibbard, K., Hurtt, G., Kram, T., Krey, V., Lamarque, J.-F., Masui, T., Meinshausen, M., Nakicenovic, N., Smith, S., Rose, S., 2011. The representative concentration pathways: an overview. *Clim. Change* 109 (1–2), 5–31.
- Vörösmarty, C.J., Fekete, B.M., Meybeck, M., Lammers, R.B., 2000. A simulated topological network representing the global system of rivers at 30-min spatial resolution (stn-30). *Global Biogeochem. Cyc.* 14, 599–621.
- Wada, Y., van Beek, L.P.H., van Kempen, C.M., Reckman, J.W.T.M., Vasak, S., Bierkens, M.F.P., 2010. Global depletion of groundwater resources. *Geophys. Res. Lett.* 37, L20402.
- Wada, Y., van Beek, L.P.H., Bierkens, M.F.P., 2011. Modelling global water stress of the recent past: on the relative importance of trends in water demand and climate variability. *Hydrol. Earth Syst. Sci.* 15 (12), 3785–3808.
- Wada, Y., van Beek, L.P.H., Viviroli, D., Drr, H.H., Weingartner, R., Bierkens, M.F.P., 2011. Global monthly water stress: 2. Water demand and severity of water stress. *Water Resour. Res.* 47 (7), W07518.
- Wada, Y., van Beek, L.P.H., Bierkens, M.F.P., 2012. Nonsustainable groundwater sustaining irrigation: a global assessment. *Water Resour. Res.* 48 (6), W00L06.
- Wada, Y., van Beek, L.P.H., Wanders, N., Bierkens, M.F.P., 2013. Human water consumption intensifies hydrological drought worldwide. *Environ. Res. Lett.* 8 (3), 034036.
- Wada, Y., Wisser, D., Bierkens, M.F.P., 2014. Global modeling of withdrawal, allocation and consumptive use of surface water and groundwater resources. *Earth Syst. Dynam.* 5, 15–40.
- Wanders, N., Van Lanen, H.A.J., 2013. Future hydrological drought across climate regions around the world modelled with a synthetic hydrological modelling approach forced by three general circulation models. *Nat. Hazards Earth Syst. Sci. Discuss.* 1, 7701–7738.
- Wanders, N., Van Lanen, H.A.J., Van Loon, A.F., 2010. Indicators for Drought Characterization on A Global Scale. *Tech. Rep. 24*. EU-WATCH.
- Wanders, N., Wada, Y., Van Lanen, H.A.J., 2014. Global hydrological droughts in the 21st century under a changing hydrological regime. *Earth Syst. Dynam. Discuss.* 5 (1), 649–681.
- Warszawski, L., Frieler, K., Huber, V., Piontek, F., Serdeczny, O., Schewe, J., 2014. The inter-sectoral impact model intercomparison project (ISIMIP): project framework. *Proc. Natl. Acad. Sci.* 111 (9), 3228–3232.
- Wilhite, D., 2000. *Drought: A Global Assessment*. Routledge.
- Wilhite, D.A., Glantz, M.H., 1985. Understanding: the drought phenomenon: the role of definitions. *Water Int.* 10 (3), 111–120.
- World Meteorological Organization, 2007. *The Role of Climatological Normals in a Changing Climate*. WCDMP-No. 61, WMO-TD/No. 1377.
- Yevjevich, V., 1967. *An Objective Approach to Definition and Investigation of Continental Hydrological Droughts*. Hydrology Papers 23, Colorado State University, Fort Collins, USA.